Clinical Interventions in Aging

Dovepress
Taylor & Francis Group

Open Access Full Text Article

ORIGINAL RESEARCH

Identification of a High Visceral Adiposity Phenotype: A Cluster Analysis-Based Stratification of NAFLD Risk in the Elderly

Zhongjun Shen[1–3,*], Qian Zhang[1,3,*], Jingjin Tao[1–3], Yuying Nie[1,3], Qi Liu[1,3], He Wang[1,3], Zhongxin Li[1,3], Chong Wang[1,3], Shuo Yang[1,3], Liyan Cui[1–3]

[1]Department of Clinical Laboratory, Peking University Third Hospital, Beijing, People's Republic of China; [2]Institute of Medical Technology, Peking University Health Science Center, Beijing, People's Republic of China; [3]Core Unit of National Clinical Research Center for Laboratory Medicine, Peking University Third Hospital, Beijing, People's Republic of China

*These authors contributed equally to this work

Correspondence: Liyan Cui, Department of Clinical Laboratory, Peking University Third Hospital, Beijing, People's Republic of China, Email cliyan@163.com

Background: Non-alcoholic fatty liver disease (NAFLD), the most prevalent chronic liver disease globally, is closely linked to obesity and metabolic dysregulation. However, the relative contributions of overall adiposity versus body fat distribution patterns to NAFLD pathogenesis, particularly in the elderly population, remain incompletely understood.

Objective: This study aimed to investigate the association between cluster-derived body composition phenotypes and NAFLD risk, and identify independent risk factors for NAFLD.

Methods: This cross-sectional study enrolled 239 elderly participants. Body composition parameters (whole-body and regional fat percentages, visceral adipose tissue (VAT) area, fat-free mass) were measured via dual-energy X-ray absorptiometry (DXA). Participants were divided into NAFLD and non-NAFLD groups by abdominal ultrasonography. Inter-group comparisons were performed with Student's t-tests and chi-square tests. Cluster analysis was applied to identify distinct body composition phenotypes. Univariate and multivariate logistic regression were used to screen independent NAFLD risk factors, and ROC curve analysis evaluated the model's predictive performance.

Results: The NAFLD group showed more prominent central obesity ($P<0.001$) and higher fat-free mass ($P<0.001$) than the non-NAFLD group, with no difference in total body fat percentage. Three phenotypes were identified: high total fat with limb-dominant distribution (C1), high visceral fat with central obesity (C2), and low total fat with symmetrical distribution (C3). C2 had the worst metabolic profile and highest NAFLD prevalence (60.5%), significantly higher than C1 (27.5%) and C3 (30.3%). Multivariate analysis identified lower HDL-C, higher BMI, elevated trunk-to-leg fat ratio, and higher albumin as independent NAFLD predictors; the four-indicator combined model had optimal predictive performance (AUC=0.803).

Conclusion: In the elderly, visceral fat accumulation and central fat distribution, rather than overall adiposity itself, are key body composition features linked to NAFLD. The high visceral fat central obesity phenotype correlates with the highest metabolic risk and NAFLD prevalence, and the trunk-to-leg fat ratio is a robust NAFLD predictor.

Keywords: non-alcoholic fatty liver disease, body composition, adipose tissue distribution, visceral fat

Introduction

Non-alcoholic fatty liver disease (NAFLD) constitutes a major and growing public health concern globally, affecting approximately 25% of the adult population.[1] In the elderly, the prevalence is particularly high, yet this population remains under-represented in clinical research. Its disease spectrum is broad, ranging from simple hepatic steatosis to progression into non-alcoholic steatohepatitis (NASH), hepatic fibrosis, cirrhosis, and even hepatocellular carcinoma. Additionally, NAFLD is closely associated with an increased risk of cardiovascular diseases.[2]

https://doi.org/10.2147/CIA.S595432
Received: 11 January 2026
Accepted: 13 April 2026
Published: 21 April 2026

Abdominal obesity, characterized by excessive accumulation of visceral adipose tissue (VAT), is a core driver of NAFLD. However, traditional indices such as body weight or body mass index (BMI) fail to fully account for NAFLD risk across all individuals. Notably, NAFLD can also occur in non-obese or even lean individuals, suggesting a distinct role of adipose tissue distribution and metabolic properties in disease pathogenesis.[3] This concept aligns with the recently proposed terminology of Metabolic Dysfunction-Associated Fatty Liver Disease (MAFLD), which emphasizes the central role of metabolic dysregulation over alcohol consumption. Visceral fat, due to its high lipolytic activity and capacity to secrete pro-inflammatory cytokines, releases metabolites directly into the liver via the portal vein, thereby promoting intrahepatic lipid deposition and inflammatory responses.[4]

Currently, gold-standard methods for assessing fat distribution, such as computed tomography (CT) and magnetic resonance imaging (MRI), offer high precision but are limited by high costs and lack of accessibility for widespread use. In contrast, bioelectrical impedance analysis (BIA) has been widely adopted in clinical and research settings owing to its non-invasive, convenient, and cost-effective nature. BIA can provide multiple metrics, including visceral fat percentage, segmental fat mass, and fat-free mass, serving as a valuable tool for elucidating the relationship between fat distribution patterns and health outcomes.[5] Among these metrics, estimated visceral adipose tissue (VAT) area directly reflects the volume of metabolically active intra-abdominal fat, which is strongly linked to hepatic insulin resistance and steatosis. Additionally, the trunk-to-leg fat ratio serves as a novel indicator of fat distribution imbalance, capturing the relative shift of adipose tissue from peripheral depots to the central region—a pattern particularly relevant in the elderly, who experience age-related fat redistribution independent of total adiposity.

Although existing research has established a strong correlation between visceral fat and NAFLD, most studies have focused on middle-aged populations, with relatively limited investigation in older adults. Aging is associated with significant alterations in body composition, including increased fat mass, decreased muscle mass (i.e., sarcopenic obesity), and a redistribution of fat from subcutaneous depots to visceral and ectopic sites.[2] These age-related changes may confer unique NAFLD risk factors in the elderly population. Therefore, a thorough exploration of the association between distinct body composition phenotypes and NAFLD risk in older adults holds significant value for early risk stratification and targeted intervention in this demographic.

Based on this background, the present study aims to: 1) compare differences in body composition and metabolic profiles between elderly NAFLD patients and non-NAFLD controls; 2) apply cluster analysis to BIA-derived body composition metrics to identify distinct body composition phenotypes within the elderly population; 3) analyze the clinical metabolic characteristics and NAFLD prevalence across these phenotypic subgroups; and 4) develop and validate a predictive model for NAFLD that integrates both body composition and traditional metabolic indicators.

Materials and Methods

Study Population and Design

This cross-sectional study consecutively enrolled elderly participants (age ≥ 60 years) undergoing health examinations at Peking University Third Hospital between June 2024 and January 2025. All participants completed detailed questionnaires, physical examinations, abdominal ultrasonography, and fasting venous blood sampling. Exclusion criteria were: 1) history of excessive alcohol consumption (males >30 g/day, females >20 g/day); 2) viral hepatitis, autoimmune liver disease, drug-induced liver injury, or other known chronic liver diseases; 3) history of malignancy; 4) severe cardiac, pulmonary, or renal dysfunction; 5) thyroid dysfunction; and 6) use of medications within the preceding 3 months that could significantly affect lipid metabolism or body weight (eg., corticosteroids, statins, weight-loss drugs). The study protocol was approved by the Ethics Committee of Peking University Third Hospital (Approval No. S2024547), and written informed consent was obtained from all participants.

Laboratory Measurements

Body Composition Assessment: Body composition was measured using dual-energy X-ray absorptiometry (DXA; Hologic QDR) under standardized conditions. Participants were assessed after fasting and voiding their bladder, wearing light clothing and no footwear. Measured parameters included: height, weight, BMI, whole-body and segmental (left/

right arm, trunk, left/right leg, abdomen, hip) fat percentages (%), whole-body fat-free mass, appendicular lean mass index, whole-body fat percentage (%), fat mass index (kg/m^2), and estimated visceral adipose tissue (VAT) area (cm^2). Derived indices included the abdominal-to-hip fat ratio, trunk-to-leg fat percentage ratio, and trunk-to-limb fat mass ratio as markers of central obesity.

Biochemical Analysis: Venous blood samples were collected from all participants after an overnight fast (≥8 hours). A fully automated biochemical analyzer was used to measure the following parameters: liver function (ALT, AST, GGT, ALP, total protein, albumin, total bilirubin, direct bilirubin); renal function (urea, creatinine, uric acid, cystatin C, estimated glomerular filtration rate [eGFR]); lipid profile (total cholesterol, triglycerides, HDL-C, LDL-C, apolipoprotein A1, apolipoprotein B, lipoprotein(a)); fasting plasma glucose; electrolytes (sodium, potassium, chloride, calcium, phosphorus); high-sensitivity C-reactive protein (hs-CRP); iron; and magnesium.

Diagnosis of Fatty Liver Disease: Abdominal ultrasonography was performed by experienced sonographers using a color Doppler ultrasound system. The sonographers were blinded to the participants' clinical and biochemical data. The diagnosis of fatty liver was made according to the ultrasound criteria outlined in the "Guidelines for the Prevention and Treatment of Non-alcoholic Fatty Liver Disease" issued by the Chinese Society of Hepatology (2018 version), which included increased echogenicity of the liver parenchyma compared to the renal cortex or spleen, and blurring of the intrahepatic vessel walls.[6]

Statistical Analysis

All statistical analyses were performed using SPSS software (version 26.0; IBM Corp.) and R software (version 4.3.1). Continuous variables with a normal distribution are presented as mean ± standard deviation, while non-normally distributed variables are presented as median (25th percentile, 75th percentile). Categorical variables are expressed as frequency (percentage). Participants were categorized into NAFLD and non-NAFLD groups based on ultrasonography findings. Group comparisons for continuous variables were performed using independent samples t-tests or Mann–Whitney *U*-tests, as appropriate. Categorical variables were compared using chi-square tests.

To identify distinct body composition phenotypes, an exploratory hierarchical cluster analysis using Ward's linkage method and squared Euclidean distance was performed on key body composition indicators, including whole-body and major segmental fat percentages, VAT area, fat-free mass index, and related ratios. All continuous variables were standardized (z scores) prior to analysis to avoid scale bias. The optimal number of clusters was determined by inspecting the dendrogram and the elbow method based on within-cluster sum of squares.

Differences in clinical and metabolic characteristics among the identified clusters were compared using one-way analysis of variance (ANOVA) or the Kruskal–Wallis test, with post-hoc pairwise comparisons adjusted using the Bonferroni method. To explore independent clinical factors distinguishing the different body composition phenotypes, multinomial logistic regression analysis was conducted, using the most common phenotype as the reference category.

To identify independent risk factors for NAFLD, univariate logistic regression was first performed, with variables showing a significance level of $P< 0.10$ selected as candidates for the multivariate model. Subsequently, a multivariate logistic regression model was constructed using a forward stepwise selection procedure based on the likelihood ratio test.

Multicollinearity among predictor variables was assessed using the variance inflation factor (VIF). The discriminatory ability of the final multivariate model and its key predictors was evaluated by constructing receiver operating characteristic (ROC) curves and calculating the area under the curve (AUC) with its 95% confidence interval (CI). The correlation between key body composition indicators (eg., VAT area, trunk-to-limb fat ratio) and major metabolic parameters was examined using Pearson or Spearman correlation analysis, as appropriate. All statistical tests were two-sided, and a *P* value of less than 0.05 was considered statistically significant.The methodology was informed by previous studies employing similar body composition parameters in the context of NAFLD research.[7]

Results

Baseline Characteristics of the Study Population

A total of 239 participants were enrolled in the present study. The mean age of the study population was 74.29 ± 8.98 years, with 137 females (57.32%). Based on abdominal ultrasonography, 82 participants (34.31%) were diagnosed with non-alcoholic fatty liver disease (NAFLD). Detailed demographic characteristics, body composition parameters, and laboratory biochemical profiles of the study cohort are summarized in Table 1.

Table 1 Baseline Characteristics of the Study Population (N=239)

Category	Indicator	Mean ± Standard Deviation	Median (P25, P75)
Demographic Characteristics	Age (years)	74.29 ± 8.98	76.0 (65.0, 81.0)
Basic Anthropometric Measurements	Height (cm)	162.88 ± 8.39	162.0 (157.0, 169.0)
	Weight (kg)	64.09 ± 10.50	64.0 (56.2, 70.0)
	BMI (kg/m^2)	24.06 ± 2.80	23.9 (22.3, 25.9)
Body Composition - Adiposity Indices	Total Body Fat %	36.70 ± 6.52	36.9 (31.8, 42.0)
	Left Arm Fat %	41.61 ± 9.83	42.4 (32.4, 48.6)
	Right Arm Fat %	41.00 ± 9.26	40.9 (33.4, 48.5)
	Trunk Fat %	36.63 ± 6.91	36.9 (32.2, 41.3)
	Left Leg Fat %	36.96 ± 7.71	36.3 (30.7, 42.9)
	Right Leg Fat %	37.48 ± 7.61	37.0 (31.7, 43.4)
	Abdominal Fat %	40.81 ± 7.43	41.1 (36.0, 45.7)
	Hip Fat %	37.57 ± 6.62	37.6 (32.4, 42.9)
	Head Fat %	26.75 ± 0.46	26.7 (26.5, 27.0)
	FHI (kg/m^2)	9.28 ± 2.37	9.13 (7.72, 10.70)
	VAT Area (cm^2)	135.96 ± 51.08	130.0 (103.0, 166.0)
	A/H Ratio	1.10 ± 0.16	1.09 (1.00, 1.20)
	Trunk/Leg Fat % Ratio	1.00 ± 0.14	0.99 (0.90, 1.08)
	Trunk/Limb Fat Mass Ratio	1.16 ± 0.24	1.16 (1.00, 1.28)
Body Composition - Lean Mass Indices	WB-FFMI (kg/m^2)	15.10 ± 1.88	15.0 (13.6, 16.5)
	ALMI (kg/m^2)	6.17 ± 0.98	6.08 (5.38, 6.93)
Hepatic Function Panel	ALT (U/L)	19.83 ± 9.24	18.0 (14.0, 24.0)
	AST (U/L)	24.91 ± 7.73	23.0 (20.0, 28.0)
	Total Bilirubin (μmol/L)	16.81 ± 5.66	15.9 (13.1, 18.9)
	Direct Bilirubin (μmol/L)	1.98 ± 0.95	1.8 (1.4, 2.3)
	ALP (U/L)	77.75 ± 19.20	77.0 (63.0, 88.0)
	GGT (U/L)	23.02 ± 11.43	20.0 (16.0, 27.0)
	Total Protein (g/L)	72.41 ± 4.11	72.0 (69.9, 74.7)
	Albumin (g/L)	44.40 ± 2.40	44.5 (42.8, 46.1)
	Globulin (g/L)	28.05 ± 3.94	28.0 (25.0, 30.0)
Renal Function Panel	Urea (mmol/L)	5.66 ± 1.45	5.6 (4.6, 6.4)
	Creatinine (μmol/L)	77.88 ± 12.95	76.0 (68.0, 86.0)
	eGFR (mL/min)	74.44 ± 11.56	74.0 (67.0, 83.0)
	Cystatin C (mg/L)	0.92 ± 0.20	0.89 (0.79, 1.00)
	Uric Acid (μmol/L)	338.04 ± 78.02	334.0 (291.0, 385.0)
Lipid Profile	Total Cholesterol (mmol/L)	4.64 ± 0.93	4.59 (4.01, 5.27)
	Triglycerides (mmol/L)	1.54 ± 0.89	1.33 (1.00, 1.79)
	HDL-C (mmol/L)	1.28 ± 0.29	1.26 (1.04, 1.48)
	LDL-C (mmol/L)	2.73 ± 0.78	2.72 (2.15, 3.30)
	ApoA1 (g/L)	1.59 ± 0.26	1.59 (1.38, 1.76)
	ApoB (g/L)	0.84 ± 0.21	0.81 (0.70, 0.97)
	Lp(a) (mg/L)	188.78 ± 216.91	95.0 (55.0, 222.0)

(*Continued*)

Table 1 (Continued).

Category	Indicator	Mean ± Standard Deviation	Median (P25, P75)
Glucose and Electrolytes	Glucose (mmol/L)	5.51 ± 0.89	5.30 (5.00, 5.80)
	Na (mmol/L)	139.38 ± 2.25	139.0 (138.0, 141.0)
	K (mmol/L)	4.26 ± 0.33	4.25 (4.03, 4.45)
	Cl (mmol/L)	104.95 ± 2.46	105.0 (104.0, 106.0)
	Ca (mmol/L)	2.42 ± 0.08	2.40 (2.37, 2.47)
	Phosphorus (mmol/L)	1.11 ± 0.15	1.11 (1.02, 1.22)
Other Laboratory Parameters	hs-CRP (mg/L)	1.48 ± 2.37	0.76 (0.35, 1.51)
	Fe (μmol/L)	19.78 ± 5.56	19.1 (16.0, 23.0)
	Mg (mmol/L)	0.90 ± 0.06	0.90 (0.86, 0.93)

Abbreviations: ALT, Alanine Aminotransferase; AST, Aspartate Aminotransferase; ALP, Alkaline Phosphatase; GGT, γ-Glutamyl Transferase; eGFR, Estimated Glomerular Filtration Rate; HDL-C, High-Density Lipoprotein Cholesterol; LDL-C, Low-Density Lipoprotein Cholesterol; ApoA1, Apolipoprotein A1; ApoB, Apolipoprotein B; Lp(a), Lipoprotein(a); hs-CRP, High-Sensitivity C-Reactive Protein; BMI, Body Mass Index; VAT, Visceral Adipose Tissue (Est. VAT = Estimated Visceral Adipose Tissue); A/H Ratio, Abdominal-to-Hip (Fat) Ratio; WB-FFMI, Whole Body Fat-Free Mass Index; ALMI, Appendicular Lean Mass Index.

Comparison of Characteristics Between Participants with and without Fatty Liver

A total of 239 participants were included and categorized into two groups based on abdominal ultrasonographic findings: 157 without fatty liver (non-NAFLD group) and 82 with fatty liver (NAFLD group). A comparison of demographic characteristics, laboratory biochemical markers, and body composition parameters between the two groups is presented in Table 2.

Table 2 Comparison of Characteristics Between Participants with and without Fatty Liver (Mean ± SD)

	Fatty Liver Disease (0=No; 1=Yes) (Mean±SD)		*t*	*P*
	0.0 (n=149)	1.0 (n=82)		
Age	75.45±8.64	72.22±9.31	2.645	0.009**
ALT	18.72±8.35	21.61±10.14	−2.325	0.021*
AST	24.77±7.20	25.10±8.52	−0.308	0.759
Total Bilirubin	16.90±5.90	16.49±4.81	0.539	0.591
Direct Bilirubin	1.93±0.82	2.09±1.17	−1.206	0.229
ALP	77.21±19.76	78.48±18.49	−0.477	0.634
Total Protein	72.12±4.00	72.85±4.23	−1.299	0.195
Albumin	44.05±2.36	44.98±2.36	−2.885	0.004**
GGT	21.09±9.49	25.70±12.98	−3.088	0.002**
Globulin	28.12±4.14	27.94±3.44	0.338	0.735
Urea	5.71±1.55	5.55±1.29	0.811	0.418
Creatinine	78.12±12.86	77.55±13.67	0.316	0.752
Calcium	2.41±0.08	2.42±0.08	−0.486	0.628
Phosphorus	1.12±0.14	1.10±0.16	0.749	0.455
Uric Acid	331.01±76.31	347.50±81.32	−1.536	0.126
eGFR	72.96±10.38	76.98±13.21	−2.367	0.019*
Total Cholesterol	4.60±0.89	4.62±0.95	−0.180	0.857
Triglycerides	1.33±0.66	1.90±1.14	−4.170	0.000**
HDL-C	1.36±0.29	1.14±0.24	5.775	0.000**
LDL-C	2.66±0.74	2.79±0.82	−1.203	0.230
ApoA1	1.63±0.27	1.50±0.22	3.947	0.000**
ApoB	0.81±0.20	0.88±0.21	−2.778	0.006**

(*Continued*)

https://doi.org/10.2147/CIA.S595432

Table 2 (Continued).

	Fatty Liver Disease (0=No; 1=Yes) (Mean±SD)		t	*P*
	0.0 (n=149)	**1.0 (n=82)**		
Lp(a)	217.36±238.81	148.73±171.36	2.521	0.012*
Glucose	5.35±0.73	5.76±1.01	−3.222	0.002**
hs-CRP	1.39±2.63	1.66±1.95	−0.806	0.421
Na	139.18±2.32	139.62±2.08	−1.433	0.153
K	4.26±0.31	4.26±0.36	0.040	0.968
Cl	104.89±2.46	105.06±2.55	−0.492	0.623
Cystatin C	0.91±0.19	0.92±0.22	−0.055	0.956
Fe	19.84±5.63	19.59±5.57	0.329	0.743
Mg	0.89±0.06	0.90±0.06	−0.665	0.507
Height (cm)	161.90±8.51	164.75±7.70	−2.520	0.012*
Weight (kg)	61.43±9.51	68.98±10.54	−5.550	0.000**
BMI	23.37±2.66	25.31±2.70	−5.288	0.000**
Left Arm Fat %	41.37±9.56	41.91±10.45	−0.393	0.695
Right Arm Fat %	40.73±8.99	41.41±9.99	−0.515	0.608
Trunk Fat %	35.49±6.99	38.50±6.48	−3.211	0.002**
Left Leg Fat %	37.42±8.03	36.15±7.32	1.183	0.238
Right Leg Fat %	37.80±7.92	37.02±7.34	0.733	0.464
Head Fat %	26.64±0.39	26.91±0.52	−4.093	0.000**
Abdominal Fat %	39.41±7.53	43.21±6.53	−3.835	0.000**
Hip Fat %	37.76±6.83	37.20±6.46	0.610	0.543
Total Body Fat %	36.19±6.65	37.54±6.43	−1.495	0.136
Fat Height % (kg/m^2)	8.90±2.33	9.97±2.38	−3.305	0.001**
A/H Ratio	1.05±0.15	1.17±0.14	−6.149	0.000**
Trunk/Leg Fat % Ratio	0.95±0.13	1.07±0.12	−6.124	0.000**
Trunk/Limb Fat Mass Ratio	1.09±0.21	1.27±0.22	−6.153	0.000**
Est. VAT Mass (g)	579.13±221.32	784.67±236.07	−6.595	0.000**
Est. VAT Volume (cm^3)	626.09±239.25	848.33±255.18	−6.597	0.000**
Est. VAT Area (cm^2)	120.09±45.89	162.77±48.93	−6.607	0.000**
WB-FFMI	14.78±1.76	15.72±1.98	−3.732	0.000**
ALMI	6.03±0.93	6.46±1.01	−3.205	0.002**

Notes: *$P<0.05$ **$P<0.01$.

Abbreviations: ALT, Alanine Aminotransferase; AST, Aspartate Aminotransferase; ALP, Alkaline Phosphatase; GGT, γ-Glutamyl Transferase; eGFR, Estimated Glomerular Filtration Rate; HDL-C, High-Density Lipoprotein Cholesterol; LDL-C, Low-Density Lipoprotein Cholesterol; ApoA1, Apolipoprotein A1; ApoB, Apolipoprotein B; Lp(a), Lipoprotein(a); hs-CRP, High-Sensitivity C-Reactive Protein; BMI, Body Mass Index; VAT, Visceral Adipose Tissue (Est. VAT = Estimated Visceral Adipose Tissue); A/H Ratio, Abdominal-to-Hip (Fat) Ratio; WB-FFMI, Whole Body Fat-Free Mass Index; ALMI, Appendicular Lean Mass Index.

The mean age of participants in the NAFLD group was significantly younger than that in the non-NAFLD group (P=0.009). However, their body weight and body mass index were significantly higher (both P<0.001). Regarding metabolic profiles, the NAFLD group exhibited significantly elevated levels of serum triglycerides, fasting plasma glucose, and apolipoprotein B, alongside significantly reduced levels of high-density lipoprotein cholesterol (HDL-C) and apolipoprotein A1 (all P<0.01). Among liver function indicators, alanine aminotransferase (ALT) and gamma-glutamyl transferase (GGT) levels were significantly higher in the NAFLD group (both P<0.05), while albumin levels were also slightly higher (P=0.004).

Although there was no significant difference in total body fat percentage between the two groups (P=0.136), distinct patterns of fat distribution were observed. The NAFLD group demonstrated a pronounced central obesity phenotype, characterized by significantly higher trunk fat percentage and abdominal fat percentage compared to the non-NAFLD group (both P<0.01). Indices reflecting central fat accumulation, such as the abdominal-to-hip fat ratio and the trunk-to-

limb fat mass ratio, were also significantly greater in the NAFLD group (both $P<0.001$). Notably, the estimated visceral adipose tissue (VAT) area was significantly larger in the NAFLD group ($P<0.001$). Concurrently, the whole body fat-free mass index was also significantly higher in participants with fatty liver ($P<0.001$).

In summary, within this study population, the presence of fatty liver was closely associated with younger age, higher BMI, a specific dyslipidemia profile (high triglycerides and low HDL-C), elevated fasting glucose, and unique alterations in body composition. These alterations were characterized by a pattern of fat distribution favoring the trunk and visceral compartments, independent of overall adiposity, and were accompanied by higher fat-free mass.

Cluster Analysis Based on Body Composition and Phenotype Characteristics

Cluster analysis of the 239 participants identified three distinct body composition phenotypes (Cluster 1, 2, 3). All body composition and fat distribution parameters differed significantly among the three groups (all $P<0.001$), as detailed in Table 3.

The three clusters represented a gradient of overall adiposity levels. Cluster 1 (High Total Fat, Limb Fat-Dominant Phenotype, n=120): This cluster had the highest total body fat percentage and the highest fat percentages in the limbs and hips. However, its trunk fat percentage and visceral fat indices were at intermediate levels. Its fat distribution ratios (eg., abdominal-to-hip ratio) were relatively low. Cluster 2 (High Visceral Fat, Central Obesity Phenotype, n=43): The most prominent feature of this cluster was an extremely high level of visceral fat, along with the highest abdominal-to-hip fat ratio and trunk-to-limb fat mass ratio, indicating a typical central obesity pattern. Its total body fat percentage was lower than that of Cluster 1. Cluster 3 (Low Total Fat, Symmetrical Low-Fat Phenotype, n=76): This cluster exhibited the lowest values across all adiposity-related indicators, including the lowest total body fat percentage, trunk fat percentage, and visceral fat levels.

Furthermore, significant differences in fat-free mass were observed among the three clusters. Cluster 2 not only had the highest visceral fat but also exhibited significantly higher whole-body and appendicular fat-free mass indices compared to the other two clusters. Additionally, the whole-body fat-free mass index of Cluster 3 was significantly higher than that of Cluster 1.

Table 3 Cluster Analysis Based on Body Composition Characteristics and Inter-Group Comparisons

	Cluster_1 (n=120)	**Cluster_2 (n=43)**	**Cluster_3 (n=76)**	***F***	***P***
Left Arm Fat %	48.60±6.09	39.70±8.73	31.67±4.98	168.438	0.000
Right Arm Fat %	47.39±5.91	39.67±8.30	31.64±4.81	156.374	0.000
Trunk Fat %	40.24±4.59	39.83±5.46	29.13±4.21	145.665	0.000
Left Leg Fat %	42.59±5.20	34.35±5.91	29.56±4.04	165.024	0.000
Right Leg Fat %	42.90±5.25	34.77±5.90	30.46±4.41	144.490	0.000
Head Fat %	26.77±0.43	27.11±0.44	26.50±0.34	32.509	0.000
Abdominal Fat %	43.48±5.53	46.02±5.14	33.64±5.73	97.104	0.000
Hip Fat %	42.28±4.16	36.20±5.19	30.90±3.84	168.467	0.000
Total Body Fat %	40.98±4.01	37.42±5.33	29.55±3.48	179.708	0.000
Fat Height % (kg/m^2)	10.27±1.98	10.46±2.15	7.06±1.30	83.197	0.000
A/H Ratio	1.03±0.11	1.28±0.11	1.09±0.16	59.896	0.000
Trunk/Leg Fat % Ratio	0.95±0.12	1.16±0.11	0.98±0.13	53.268	0.000
Trunk/Limb Fat Mass Ratio	1.10±0.21	1.43±0.17	1.10±0.21	47.278	0.000
Est. VAT Mass (g)	586.15±164.25	1040.00±186.05	547.65±161.59	139.304	0.000
Est. VAT Volume (cm^3)	633.67±177.54	1124.30±201.15	592.06±174.66	139.323	0.000
Est. VAT Area (cm^2)	121.55±34.08	215.65±38.54	113.62±33.54	139.092	0.000
WB-FFMI	14.01±1.28	16.62±1.79	15.97±1.69	65.498	0.000
ALMI	5.54±0.62	6.88±0.91	6.76±0.83	85.291	0.000

https://doi.org/10.2147/CIA.S595432

Differences in Clinical and Metabolic Indicators Among Different Body Composition Subgroups

Following the identification of three body composition subgroups with distinct fat distribution patterns—high total fat, limb-dominant (Cluster 1); high visceral fat, central obesity (Cluster 2); and low total fat, symmetrical low-fat (Cluster 3)—we further analyzed differences in demographic characteristics, liver and kidney function, and glucose/lipid metabolism among these subgroups (Table 4). Results of post-hoc pairwise comparisons (adjusted for multiple comparisons) are detailed in Table S1.

Significant differences were observed in demographic and anthropometric indicators among the three groups. The high visceral fat, central obesity group (Cluster 2) had the youngest age but the tallest height, greatest body weight, and highest BMI (all $P<0.001$). The high total fat, limb-dominant group (Cluster 1) was the oldest, but had significantly lower height and body weight compared to the other two groups. The low total fat, symmetrical low-fat group (Cluster 3) had an intermediate age and the lowest body weight; however, its BMI was not significantly different from that of Cluster 1 but was significantly lower than that of Cluster 2.

Table 4 Differences in Clinical and Metabolic Indicators Among Different Body Composition Subgroups

	Cluster_1 (n=120)	Cluster_2 (n=43)	Cluster_3 (n=76)	*F*	*P*
Age	75.83±9.07	71.88±9.07	73.22±8.42	3.946	0.021*
ALT	18.87±8.68	22.37±11.79	19.91±8.27	2.307	0.102
AST	25.26±8.27	25.00±9.03	24.30±5.90	0.358	0.700
Total Bilirubin	15.49±3.99	17.45±7.31	18.53±6.35	7.405	0.001**
Direct Bilirubin	1.86±1.07	2.05±0.85	2.12±0.78	1.879	0.155
ALP	80.63±21.26	77.65±14.65	73.26±17.28	3.502	0.032*
Total Protein	72.36±3.70	72.75±4.67	72.29±4.42	0.184	0.832
Albumin	44.07±2.51	44.85±2.14	44.69±2.30	2.502	0.084
GGT	22.43±12.38	26.72±10.42	21.84±10.03	2.862	0.059
Globulin	28.35±3.36	27.93±3.77	27.66±4.81	0.741	0.478
Urea	5.56±1.38	5.93±1.27	5.68±1.64	0.998	0.370
Creatinine	71.61±8.81	80.84±13.67	86.11±12.97	40.679	0.000**
Calcium	2.42±0.09	2.41±0.07	2.41±0.08	0.463	0.630
Phosphorus	1.16±0.13	1.10±0.17	1.05±0.13	14.756	0.000**
Uric Acid	312.02±65.52	362.88±80.82	365.07±81.68	14.991	0.000**
eGFR	72.99±11.03	77.23±12.40	75.12±11.69	2.345	0.098
Total Cholesterol	4.76±0.98	4.56±0.95	4.49±0.80	2.060	0.130
Triglycerides	1.43±0.59	2.16±1.46	1.38±0.71	14.036	0.000**
HDL-C	1.34±0.29	1.11±0.24	1.27±0.29	10.707	0.000**
LDL-C	2.78±0.81	2.67±0.85	2.69±0.70	0.455	0.635
ApoA1	1.64±0.27	1.50±0.22	1.55±0.24	6.189	0.002**
ApoB	0.85±0.22	0.86±0.21	0.82±0.18	0.873	0.419
Lp(a)	231.39±241.79	116.56±122.36	162.37±203.85	5.460	0.005**
Glucose	5.47±0.81	5.90±1.21	5.35±0.73	5.707	0.004**
hs-CRP	1.64±2.81	1.68±1.81	1.13±1.81	1.271	0.282
Na	139.68±2.38	139.19±1.98	139.00±2.15	2.358	0.097
K	4.26±0.31	4.32±0.38	4.23±0.32	0.921	0.399
Cl	105.18±2.20	105.02±2.52	104.54±2.77	1.627	0.199
Cystatin C	0.89±0.16	0.96±0.22	0.93±0.23	1.921	0.149
Fe	19.02±4.72	19.13±5.45	21.33±6.52	4.478	0.012*
Mg	0.90±0.06	0.90±0.07	0.89±0.06	0.545	0.581
Height (cm)	157.77±6.06	167.81±6.28	168.16±7.66	71.257	0.000**
Weight (kg)	59.44±7.72	73.74±9.88	65.96±10.44	41.829	0.000**
BMI	23.86±2.65	26.13±2.84	23.20±2.45	17.929	0.000**

Note: * $P<0.05$ ** $P<0.01$.

https://doi.org/10.2147/CIA.S595432

Cluster 2 displayed the most unfavorable metabolic profile, with levels of alanine aminotransferase (ALT), gamma-glutamyl transferase (GGT), triglycerides, and fasting plasma glucose significantly higher than those in Cluster 1 and/or Cluster 3 (all $P<0.05$), while its high-density lipoprotein cholesterol (HDL-C) and apolipoprotein A1 levels were the lowest. In contrast, Cluster 1 possessed a relatively more favorable lipid profile, with the highest levels of HDL-C and apolipoprotein A1.

Serum creatinine levels were highest in Cluster 3, followed by Cluster 2, and were lowest in Cluster 1 (pairwise comparisons among all three groups were $P<0.05$). Consistently, the estimated glomerular filtration rate (eGFR) was lowest in Cluster 1. Uric acid levels were significantly higher in both Cluster 2 and Cluster 3 compared to Cluster 1 (both $P<0.001$).

Additionally, serum phosphorus and lipoprotein(a) levels were highest in Cluster 1. Serum iron levels were significantly higher in Cluster 3 than in the other two groups.

The three body composition phenotypes revealed by cluster analysis not only exhibited distinct fat distribution patterns but also displayed specific accompanying clinical and metabolic characteristics. The high visceral fat, central obesity phenotype (Cluster 2) integrated the greatest number of cardiometabolic risk factors, including higher BMI, blood glucose, triglycerides, liver enzymes, and lower HDL-C. Conversely, the high total fat, limb-dominant phenotype (Cluster 1), despite having the highest total adiposity, demonstrated a relatively more moderate metabolic risk profile.

Association Between Body Composition Phenotypes and Prevalence of Fatty Liver Disease

To investigate the relationship between different body composition phenotypes and the risk of fatty liver disease (FLD), a chi-square test was performed. As shown in Table 5, a highly significant difference was observed in the distribution of FLD prevalence among the three body composition subgroups ($\chi^2 = 16.073$, $P < 0.001$).

The prevalence of FLD was significantly higher in individuals with the high visceral fat and central obesity phenotype (Cluster 2), reaching 60.5%. In contrast, FLD prevalence rates were similar in the high total fat with limb-dominant distribution phenotype (Cluster 1) and the low total fat with symmetrical distribution phenotype (Cluster 3), at 27.5% and 30.3%, respectively.

These findings further confirm that excessive visceral fat accumulation, rather than elevated total body fat alone, is strongly associated with the development of FLD. The Cluster 2 phenotype, which is characterized by the most unfavorable metabolic profile, also represents the subgroup with the highest risk of FLD.

Analysis of Independent Factors Distinguishing Different Body Composition Phenotypes

To identify the core clinical indicators that determine different body composition phenotypes, we performed multinomial logistic regression analysis using the most common phenotype—high total fat, limb-dominant (Cluster 1)—as the reference category (Table 6).

Independent Characteristics of the High Visceral Fat, Central Obesity Phenotype (Cluster 2): After adjusting for multiple parameters, hypertriglyceridemia emerged as the strongest factor distinguishing Cluster 2 from Cluster

Table 5 Prevalence of Fatty Liver Disease Across Different Body Composition Phenotypes

Body Composition Subtype	Non-Fatty Liver (n=157)	Fatty Liver (n=82)	Total	Fatty Liver Prevalence
Cluster 1: High Overall Adiposity with Limb-Dominant Fat Distribution	87 (72.5%)	33 (27.5%)	120	27.50%
Cluster 2: High Visceral Adiposity with Central Obesity Pattern	17 (39.5%)	26 (60.5%)	43	60.50%
Cluster 3: Low Overall Adiposity with Symmetrically Low Fat	53 (69.7%)	23 (30.3%)	76	30.30%

1 (OR = 3.72, 95% CI: 1.45–9.57, P= 0.006). Additionally, a higher serum total bilirubin level (OR = 1.15, P= 0.030) was independently associated with the Cluster 2 phenotype.

Independent Characteristics of the Low Total Fat, Symmetrical Low-Fat Phenotype (Cluster 3): Cluster 3 represents a unique "tall and lean" morphotype. Greater height (OR = 0.41, P= 0.003) and an extremely low BMI (OR = 0.015, P< 0.001) were its primary distinguishing features, indicating that individuals who are taller and have a lower body fat percentage for a given weight are more likely to belong to this phenotype. Concurrently, this group was associated with higher serum creatinine (OR = 1.11, P< 0.001) and lower serum phosphorus levels (OR = 0.011, P= 0.010).

This analysis indicates that dyslipidemia (elevated triglycerides) is a core metabolic marker distinguishing the visceral fat-accumulating phenotype (Cluster 2), while a distinct physique (tall and lean body type) is the primary determinant of the low-fat phenotype (Cluster 3). These findings further validate that the phenotypes derived from cluster analysis possess distinct clinical and physiological underpinnings.

Table 6 Multinomial Logistic Regression Analysis for Distinguishing Different Body Composition Phenotypes

Cluster_2	**Regression Coefficient**	**Standard Error**	***z Value***	**Wald χ^2**	***P* value**	**Odds Ratio (OR)**	**95% CI for OR**
Age	−0.036	0.034	−1.044	1.091	0.296	0.965	0.903 ~ 1.032
Total Bilirubin	0.136	0.063	2.171	4.712	0.030	1.145	1.013 ~ 1.295
ALP	−0.000	0.014	−0.034	0.001	0.973	1.000	0.972 ~ 1.028
Creatinine	0.044	0.028	1.567	2.457	0.117	1.045	0.989 ~ 1.104
Phosphorus	−2.792	1.926	−1.450	2.101	0.147	0.061	0.001 ~ 2.672
Uric Acid	0.004	0.004	0.976	0.952	0.329	1.004	0.996 ~ 1.012
Triglycerides	1.314	0.482	2.727	7.435	0.006	3.721	1.447 ~ 9.568
HDL-C	0.756	3.318	0.228	0.052	0.820	2.131	0.003 ~ 1422.483
ApoA1	−0.725	3.062	−0.237	0.056	0.813	0.485	0.001 ~ 195.866
Lp(a)	−0.002	0.002	−1.226	1.502	0.220	0.998	0.994 ~ 1.001
Glucose	0.315	0.302	1.042	1.087	0.297	1.370	0.758 ~ 2.477
Fe	−0.094	0.055	−1.713	2.933	0.087	0.910	0.818 ~ 1.014
Height (cm)	−0.453	0.415	−1.090	1.189	0.276	0.636	0.282 ~ 1.435
Weight (kg)	0.895	0.520	1.723	2.968	0.085	2.449	0.884 ~ 6.782
BMI	−2.018	1.380	−1.462	2.138	0.144	0.133	0.009 ~ 1.988
Intercept	61.159	68.043	0.899	0.808	0.369	3.6376435186643876e+26	0.000 ~ 3.0118226728789318e+84
Cluster_3	**Regression Coefficient**	**Standard Error**	***z Value***	**Wald χ^2**	***P* value**	**Odds Ratio (OR)**	**95% CI for OR**
Age	−0.045	0.030	−1.488	2.214	0.137	0.956	0.901 ~ 1.014
Total Bilirubin	0.108	0.054	2.003	4.012	0.045	1.114	1.002 ~ 1.238
ALP	−0.008	0.013	−0.576	0.331	0.565	0.992	0.967 ~ 1.018
Creatinine	0.100	0.027	3.698	13.674	0.000	1.106	1.048 ~ 1.166
Phosphorus	−4.525	1.763	−2.567	6.590	0.010	0.011	0.000 ~ 0.343
Uric Acid	0.007	0.004	1.678	2.816	0.093	1.007	0.999 ~ 1.015
Triglycerides	0.651	0.460	1.414	2.000	0.157	1.917	0.778 ~ 4.722
HDL-C	3.914	2.963	1.321	1.745	0.186	50.083	0.151 ~ 16,653.094
ApoA1	−3.505	2.867	−1.222	1.494	0.222	0.030	0.000 ~ 8.293
Lp(a)	−0.002	0.001	−1.504	2.262	0.133	0.998	0.995 ~ 1.001
Glucose	0.085	0.295	0.289	0.083	0.773	1.089	0.611 ~ 1.942
Fe	−0.026	0.051	−0.509	0.259	0.610	0.975	0.883 ~ 1.076
Height (cm)	−0.902	0.300	−3.003	9.018	0.003	0.406	0.225 ~ 0.731
Weight (kg)	1.459	0.407	3.583	12.840	0.000	4.304	1.937 ~ 9.562
BMI	−4.173	1.078	−3.872	14.995	0.000	0.015	0.002 ~ 0.127
Intercept	150.261	48.495	3.099	9.601	0.002	1.8085050561329602e+65	9.520431785619433e+23 ~ 3.435443487971674e+106

Note: McFadden R^2 = 0.497; Cox & Snell R^2 = 0.636; Nagelkerke R^2 = 0.732.

Correlation Analysis Between Visceral Adiposity and Metabolic Parameters

To investigate the relationships between key body composition indicators and clinical metabolic parameters, a correlation analysis was conducted (Table 7).

Strong correlations were observed between visceral adiposity and metabolic risk factors. The estimated visceral adipose tissue area (Est.VAT Area) showed significant positive correlations with several metabolic risk markers, including fasting plasma glucose (r = 0.232, $P< 0.01$), triglycerides (r = 0.266, $P< 0.01$), gamma-glutamyl transferase (GGT; r = 0.298, $P< 0.01$), and high-sensitivity C-reactive protein (hs-CRP; r = 0.205, $P< 0.01$). Conversely, a significant negative correlation was found with high-density lipoprotein cholesterol (HDL-C; r = −0.315, $P< 0.01$).

Central obesity indicators were associated with dyslipidemia. Indices reflecting a central fat distribution pattern, such as the abdominal-to-hip fat ratio and the trunk-to-limb fat mass ratio, were positively correlated with triglycerides (r = 0.257 and 0.249, respectively; both $P< 0.01$) and fasting plasma glucose (r = 0.204 and 0.214, respectively; both $P< 0.01$). Both ratios were negatively correlated with HDL-C (r = −0.361 and −0.342, respectively; both $P< 0.01$). Furthermore, total body fat percentage was negatively correlated with serum uric acid levels (r = −0.189, $P< 0.01$).

The correlation analysis indicates that visceral fat accumulation and a central obesity distribution pattern, rather than a simple increase in overall adiposity, are more closely linked to glucose and lipid metabolism abnormalities, elevated liver enzymes, and a low-grade inflammatory state. This provides quantitative evidence for understanding the metabolic risks associated with different body composition phenotypes, particularly the high visceral fat phenotype.

Multivariate Analysis of Risk Factors for Fatty Liver Disease

To construct a predictive model for fatty liver disease (FLD), a multi-stage variable selection strategy was employed. First, univariate analysis was performed on all candidate variables from Comparison of Characteristics Between Participants With and Without Fatty Liver, identifying 26 variables significantly associated with FLD at a threshold of $P<0.10$. Subsequent collinearity diagnostics revealed severe multicollinearity issues, leading to the identification of five highly correlated variable groups (Tables S2, S3 and S4). Through systematic variable selection based on variance inflation factor (VIF) analysis and clinical importance assessment, a predictive model with significant findings was developed (Table 8). This model incorporates four highly significant predictors:

The trunk-to-leg fat ratio demonstrated remarkable predictive power (OR = 76.941, 95% CI: 7.124–830.991, $P<0.001$), indicating that each 0.1-unit increase elevates FLD risk by approximately 76.9-fold. HDL-C provided strong metabolic protection (OR = 0.092, 95% CI: 0.025–0.340, $P<0.001$). BMI, as a measure of overall obesity, showed a significant risk effect (OR = 1.237, 95% CI: 1.096–1.397, $P=0.001$). Albumin maintained a consistent but modest risk contribution (OR = 1.158, 95% CI: 1.009–1.330, $P=0.037$).

Table 7 Correlations Between Core Body Composition Indicators and Major Metabolic Risk Markers

Metabolic Risk Indices	Estimated Visceral Adipose Tissue Area (cm^2)	Abdominal-to-Hip Fat Ratio	Trunk-to-Limb Fat Mass Ratio	Total Body Fat Percentage (%)
Fasting Plasma Glucose (mmol/L)	0.232**	0.204**	0.214**	0.109
Triglycerides (mmol/L)	0.266**	0.257**	0.249**	0.135*
HDL-C (mmol/L)	−0.315**	−0.361**	−0.342**	0.098
LDL-C (mmol/L)	−0.008	0.103	0.111	0.116
ApoB (g/L)	0.026	0.182**	0.194**	0.129*
ALT (U/L)	0.088	0.153*	0.157*	−0.066
GGT (U/L)	0.298**	0.273**	0.286**	0.01
hs-CRP (mg/L)	0.205**	0.099	0.108	0.170**
Serum Creatinine (μmol/L)	0.094	0.172**	0.043	−0.464**
Uric Acid (μmol/L)	0.253**	0.259**	0.159*	−0.189**

Note: *$P<0.05$ **$P<0.01$.

https://doi.org/10.2147/CIA.S595432

Table 8 Multivariate Analysis of Risk Factors for Fatty Liver Disease

Variable	Regression Coefficient	Standard Error	z Value	Wald χ^2	*P* value	Odds Ratio (OR)	95% Confidence Interval for OR
HDL-C	−2.381	0.664	−3.583	12.839	0.000	0.092	0.025 ~ 0.340
BMI	0.213	0.062	3.429	11.761	0.001	1.237	1.096 ~ 1.397
Trunk/Leg Fat % Ratio	4.343	1.214	3.577	12.796	0.000	76.941	7.124 ~ 830.991
Albumin	0.147	0.070	2.082	4.334	0.037	1.158	1.009 ~ 1.330
Intercept	−13.843	3.831	−3.613	13.053	0.000	0.000	0.000 ~ 0.002

Notes: McFadden R^2 = 0.221. Cox & Snell R^2 = 0.248. Nagelkerke R^2 = 0.342.

The model demonstrated a goodness-of-fit with a Nagelkerke R^2 of 0.342. All included variables were statistically significant ($P<0.05$), reflecting the model's robustness.

The diagnostic performance of the predictive model was subsequently evaluated using receiver operating characteristic (ROC) curve analysis (Figure 1). The combined diagnostic model exhibited good discriminatory ability, with an area under the curve (AUC) of 0.803 (95% CI: 0.749–0.858, $P<0.001$). This indicates that the model can correctly distinguish between individuals with and without FLD in 83.0% of cases, suggesting potential for clinical application. Among individual predictors, the trunk-to-leg fat ratio performed best (AUC = 0.720, 95% CI: 0.655–0.786, $P<0.001$), further validating the critical role of imbalanced body fat distribution in predicting FLD. BMI, as a traditional obesity indicator, showed moderate diagnostic performance (AUC = 0.698, 95% CI: 0.629–0.767, $P<0.001$). Albumin had an AUC of 0.592 (95% CI: 0.515–0.668, $P=0.020$); although lower than other indicators, it remained statistically significant, supporting its supplementary value in the multivariate model. Notably, HDL-C exhibited a unique inverse predictive pattern (AUC = 0.291, 95% CI: 0.224–0.359, $P<0.001$), consistent with its known protective role, where lower levels correspond to higher disease risk. Overall, the AUC of the combined diagnostic model was significantly higher than that of any single indicator, highlighting the advantage of integrating metabolic, body composition, and biochemical parameters for multidimensional risk assessment.

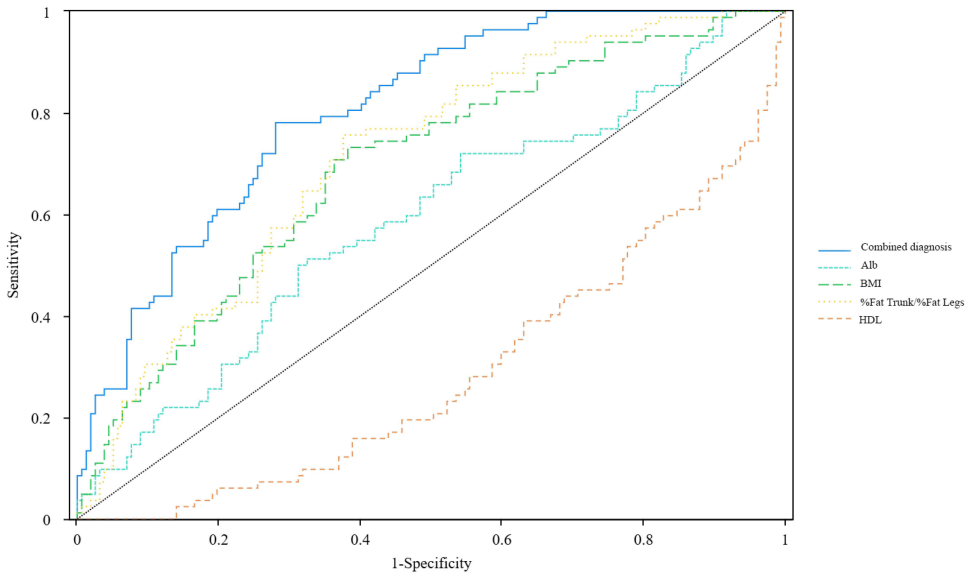

Figure 1 Receiver operating characteristic (ROC) curves of the prediction model for fatty liver disease in the elderly population.

https://doi.org/10.2147/CIA.S595432

Discussion

This study, utilizing cluster analysis of body composition, identified three distinct and heterogeneous body composition phenotypes within an elderly population and thoroughly investigated their association with the risk of non-alcoholic fatty liver disease (NAFLD). The principal findings include: (1) The occurrence of NAFLD is more closely related to visceral fat accumulation and a central fat distribution pattern than to increased total adiposity alone; (2) The "high visceral fat, central obesity phenotype" (Cluster 2) represents a high-risk subtype for NAFLD and metabolic dysregulation, with a prevalence reaching 60.5%; (3) A combined model incorporating HDL-C, BMI, trunk-to-leg fat ratio, and albumin effectively predicted NAFLD risk (AUC=0.803), with the trunk-to-leg fat ratio (AUC=0.720) demonstrating superior predictive power compared to the traditional BMI metric (AUC=0.698). These findings provide a novel perspective for understanding the pathophysiology and risk stratification of NAFLD in the elderly.

Our results emphasize that fat distribution, rather than total fat mass, is the critical dimension associated with NAFLD risk. Although no statistical difference was observed in total body fat percentage between the NAFLD and non-NAFLD groups, all indicators reflecting central obesity and visceral fat accumulation showed highly significant differences (Table 2). This finding aligns with the growing research consensus that visceral adipose tissue (VAT), due to its unique anatomical location and metabolic properties (eg., high lipolytic activity and pro-inflammatory cytokine secretion), directly impacts the liver via the portal vein, acting as a key factor associated with intrahepatic lipid deposition and insulin resistance.[8–10] In the present study, the significant positive correlations between estimated VAT area and triglycerides, fasting glucose, GGT, and hs-CRP (Correlation Analysis Between Visceral Adiposity and Metabolic Parameters) further corroborate the role of visceral fat as an important correlate for metabolic disturbances and liver injury.

Recent findings by Wang et al provide a cellular-level explanation for age-related visceral fat accumulation.[11] Using lineage tracing and single-cell RNA sequencing, the authors identified a distinct population of committed preadipocytes —termed CP-A (committed preadipocyte, age-enriched)—that emerges in visceral adipose tissue during middle age. Unlike most adult stem cells that diminish with aging, CP-As exhibit enhanced proliferative and adipogenic capacity, directly contributing to visceral fat expansion. A similar population was also identified in human visceral adipose tissue. These findings suggest that age-related visceral adiposity is actively driven by the emergence of a specialized progenitor cell population, providing a biological rationale for why fat distribution—rather than total adiposity—is a critical determinant of metabolic risk in older adults.

This mechanistic insight aligns with our observation that the "high visceral fat, central obesity phenotype" (Cluster 2) exhibited the highest NAFLD prevalence and most adverse metabolic profile. The emergence of CP-As in middle age may underlie the shift toward visceral fat accumulation seen in our elderly cohort, providing a biological rationale for why fat distribution—rather than total adiposity—is a critical determinant of metabolic risk in older adults.

Employing a data-driven approach, this study successfully identified body composition subtypes associated with varying metabolic risks, moving beyond simple classifications based solely on BMI or waist circumference. The metabolic profile of Cluster 2 (high visceral fat, central obesity) is particularly alarming: this subtype not only carries the heaviest visceral fat burden but also concurrently exhibits the highest levels of triglycerides, blood glucose, liver enzymes (ALT, GGT), and the lowest HDL-C levels (Table 4). This state of "multiple metabolic hits" aptly explains its highest NAFLD prevalence (Table 5). Interestingly, this subtype also displayed the highest whole-body and appendicular fat-free mass indices, suggesting a potential phenomenon of "muscle-fat co-gain" or "metabolically obese" phenotype, where pathological fat accumulation, particularly visceral fat, occurs alongside high muscle mass. This phenotype may be related to a vicious cycle of insulin resistance, where high muscle mass is accompanied by reduced insulin sensitivity, and abnormal fat distribution further exacerbates metabolic dysregulation.[12,13]

In contrast, Cluster 1 (high total fat, limb-dominant), while having the highest total adiposity, stores fat predominantly in the limbs and hips (subcutaneous depots), carries a relatively lower visceral fat burden, and shows lower fat distribution ratios. Consequently, it exhibits a milder metabolic profile and lower NAFLD risk. This outcome supports the "lipid storage capacity" hypothesis, which posits that subcutaneous adipose tissue, especially in peripheral depots, acts as a "metabolic sink." Its substantial lipid storage capacity helps sequester excess energy in a relatively inert form,

thereby reducing lipid overflow to visceral depots and the liver, conferring a protective effect on metabolic health.[14] Our study provides empirical support for this hypothesis in an elderly population.

One of the most innovative findings of this study is the prominent value of the trunk-to-leg fat ratio in predicting NAFLD. In the multivariate model, this ratio demonstrated an exceptionally high odds ratio (OR=76.941), and its predictive performance as a single indicator (AUC=0.720) surpassed that of the traditional BMI metric. This ratio essentially quantifies the imbalance in fat distribution between the metabolically active central body and the relatively inert peripheral compartments. An elevated ratio signifies a shift from a protective peripheral-subcutaneous fat pattern to a risky central-visceral pattern. Compared to simple measures like waist circumference or waist-to-hip ratio, this ratio may more precisely capture the relative distribution of fat between the trunk and limbs, serving as a powerful, easily calculable indicator for assessing "pathological fat distribution" with significant potential for clinical application.[15,16]

HDL-C was the strongest protective factor against NAFLD (OR=0.092), consistent with a large body of prior research. Low HDL-C is not only a manifestation of dyslipidemia but also a key marker of systemic insulin resistance and inflammatory status. Albumin, an indicator of nutritional status and liver synthetic function, showed a modest positive association with risk in our study. This may reflect the characteristics of our study population (elderly, community-based), where higher albumin levels might be associated with better nutritional intake, body weight, and muscle mass—factors themselves intricately linked to visceral fat accumulation. The precise underlying mechanism warrants further investigation. Furthermore, the highest serum creatinine levels in Cluster 3 might be related to this subtype's greatest height and relatively higher muscle mass, reminding us to interpret renal function markers in the context of body composition.

This study has several limitations. First, the cross-sectional design precludes causal inferences. Second, the clusters and predictive model are exploratory, derived from a single-center cohort, and require external validation in larger, diverse populations. Third, the visceral fat area estimated by BIA, while showing good correlation with CT measurements, remains an indirect estimation. Finally, the single-center design and the specific demographic of Chinese elderly undergoing health checks limit the generalizability of our findings to other ethnicities or clinical settings.

Conclusion

This study confirms that body composition-based fat distribution patterns are more important determinants of NAFLD risk than overall obesity in the elderly population. The identified "high visceral fat, central obesity phenotype" constitutes a high-risk subtype requiring urgent clinical attention and early intervention. The trunk-to-leg fat ratio, as a novel body fat distribution indicator, demonstrates excellent risk-predictive ability. We recommend its combined use with traditional indicators like BMI and waist circumference in clinical practice for more accurate identification of individuals at high risk for NAFLD. Future prospective, multi-center studies are essential to validate the prognostic value of these body composition phenotypes and to explore personalized intervention strategies tailored to different subtypes.

Patient and Public Involvement

No patients or members of the public were involved in the design, conduct, reporting, or dissemination of this research.

Data Sharing Statement

The datasets generated and/or analyzed during the current study are not publicly available due to protecting participant privacy and in compliance with institutional data management policies, but are available from the corresponding author on reasonable request.

Ethics Approval and Consent to Participate

This study was reviewed and approved by the Ethics Committee of Peking University Third Hospital (Approval No. S2024547). All procedures performed in studies involving human participants were in accordance with the ethical standards of the institutional and/or national research committee and with the 1964 Helsinki Declaration and its later amendments or comparable ethical standards. Informed consent was obtained from all individual participants included in the study.

Author Contributions

All authors made a significant contribution to the work reported, whether that is in the conception, study design, execution, acquisition of data, analysis and interpretation, or in all these areas; took part in drafting, revising or critically reviewing the article; gave final approval of the version to be published; have agreed on the journal to which the article has been submitted; and agree to be accountable for all aspects of the work.

Funding

This work was supported by the Natural Science Foundation of Beijing Municipality (Grant No. L246007) and the National Natural Science Foundation of China (Grant No. 62071011).

Disclosure

The authors declare that they have no competing interests.

References

1. Eslam M, Newsome PN, Sarin SK, et al. A new definition for metabolic dysfunction-associated fatty liver disease: an international expert consensus statement. *J Hepatol*. 2020;73:202–209. doi:10.1016/j.jhep.2020.03.039
2. Merli M, Berzigotti A, Zelber-Sagi S, et al. EASL clinical practice guidelines on nutrition in chronic liver disease. *J Hepatol*. 2019;70:172–193. doi:10.1016/j.jhep.2018.06.024
3. Weir NL, Nomura SO, Steffen BT, et al. Associations between omega-6 polyunsaturated fatty acids, hyperinsulinemia and incident diabetes by race/ethnicity: the multi-ethnic study of atherosclerosis. *Clin Nutr*. 2020;39:3031–3041. doi:10.1016/j.clnu.2020.01.003
4. Petersen A, Bressem K, Albrecht J, et al. The role of visceral adiposity in the severity of COVID-19: highlights from a unicenter cross-sectional pilot study in Germany. *Metabolism*. 2020;110:154317. doi:10.1016/j.metabol.2020.154317
5. Lambert L, Novak M, Siklova M, Krauzova E, Stich V, Burgetova A. Hybrid and model-based iterative reconstruction influences the volumetry of visceral and subcutaneous adipose tissue on ultra-low-dose CT. *Obesity*. 2020;28:2083–2089. doi:10.1002/oby.22945
6. Fan JG, Wei L, Zhuang H. Guidelines of prevention and treatment of nonalcoholic fatty liver disease (2018, China). *J Dig Dis*. 2019;20:163–173. doi:10.1111/1751-2980.12685
7. Akkila SS, Noel KI, Ibraheem MM. Adipose tissue elastography, anthropometric parameters and non-alcoholic fatty liver disease in obese adults: a cross-sectional study. *Al-Rafidain J Med Sci*. 2025;8:30–34. doi:10.54133/ajms.v8i2.1782
8. Conforto R, Rizzo V, Russo R, et al. Advances in body composition and gender differences in susceptibility to frailty syndrome: role of osteosarcopenic obesity. *Metabolism*. 2024;161:156052. doi:10.1016/j.metabol.2024.156052
9. Damanti S, Citterio L, Zagato L, et al. Sarcopenic obesity and pre-sarcopenia contribute to frailty in community-dwelling Italian older people: data from the FRASNET study. *BMC Geriatr*. 2024;24:24. doi:10.1186/s12877-023-04608-4
10. Lin X, Zhang J, Chu Y, Nie Q, Zhang J. Berberine prevents NAFLD and HCC by modulating metabolic disorders. *Pharmacol Ther*. 2024;254:108593.
11. Wang G, Li G, Song A, et al. Distinct adipose progenitor cells emerging with age drive active adipogenesis. *Science*. 2025;388(6745):eadj0430. doi:10.1126/science.adj0430
12. Khalil M, Di Ciaula A, Jaber N, Grandolfo R, Fiermonte F, Portincasa P. Multidimensional assessment of sarcopenia and sarcopenic obesity in geriatric patients: creatinine/cystatin C ratio performs better than sarcopenia index. *Metabolites*. 2024;14:306. doi:10.3390/metabo14060306
13. Meiliana A, Dewi NM, Defi IR, Rosdianto AM, Qiantori AA, Wijaya A. Sarcopenic obesity: the underlying molecular pathophysiology and prospect therapies. *Indonesian Biomed J*. 2024;16:292–308. doi:10.18585/inabj.v16i4.3176
14. Kim MJ, Cho YK, Kim EH, et al. Association between metabolic dysfunction-associated steatotic liver disease and myosteatosis measured by computed tomography. *J Cachexia Sarcopenia Muscle*. 2024;15:1942–1952. doi:10.1002/jcsm.13543
15. Merchant RA, Soong JTY, Morley JE. Gender differences in body composition in pre-frail older adults with diabetes mellitus. *Front Endocrinol*. 2022;13. doi:10.3389/fendo.2022.795594
16. Wan Q, Liu X, Xu J, et al. Body composition and progression of biopsy-proven non-alcoholic fatty liver disease in patients with obesity. *J Cachexia Sarcopenia Muscle*. 2024;15:2608–2617. doi:10.1002/jcsm.13605